RGNZ/MGPB

Influence of Confining Materials on Detonation Parameters of ANFO Explosive

Vječislav Bohanek[1]; Muhamed Sućeska[2]; Ivana Dobrilović[3]; Paulo Pleše[4]

[1] University of Zagreb, Faculty of Mining, Geology and Petroleum Engineering, Pierottijeva 6, 10000 Zagreb, Croatia
[2] University of Zagreb, Faculty of Mining, Geology and Petroleum Engineering, Pierottijeva 6, 10000 Zagreb, Croatia
[3] University of Zagreb, Faculty of Mining, Geology and Petroleum Engineering, Pierottijeva 6, 10000 Zagreb, Croatia
[4] DOK-ING ltd., Slavonska avenija 22 G,10000 Zagreb, Croatia

Abstract

Due to the low manufacturing cost and ease of handling, ammonium nitrate-fuel oil (ANFO) is one of the most popular mining explosives. ANFO explosive is a typical representative of non-ideal explosives, which means that its detonation properties are strongly dependent on the charge diameter and the existence and properties of the confinement. In this work, the effect of different confining materials on the detonation properties of ANFO explosive is studied experimentally, and by hydrocode simulation by varying charge diameter, and the type and thickness of the confining materials. The results show that, along with the diameter of the charge, density and thickness of the confining material have a key impact on the detonation properties. An empirical confinement model, applicable in the range $0.3 < m_C/m_E < 15$, is proposed. The model enables the estimation of detonation velocity of confined ANFO charges with a mean absolute percentage error (MAPE) of 14.25%.

Keywords:
explosives; ANFO; confinement; detonation; AUTODYN; confinement model

1. Introduction

Ammonium Nitrate (AN) and Fuel Oil (FO) explosive (ANFO) is the most used explosive for civilian applications, such as mining, construction, or explosive metalworking (**Bohanek et al., 2013 a, 2013b.**). ANFO is even used for criminal or terrorist attacks (**Hernandes et al., 2015; Kavicky et al., 2014**). The reason for the wide use of ANFO is its good blasting performance, handling safety, and low price. From a scientific point of view, ANFO explosives are interesting as a typical representative of non-ideal explosives (**Bohanek et al., 2023; Short & Jackson, 2015, Tumara et al., 2022**). Numerous research studies are devoted to determining the factors that impact the detonation properties of ANFO. The influence of AN prills (**Biessikirski et al., 2020; Buczkowski & Zygmunt, 2011; Fabin & Jarosz, 2021; Miyake et al., 2001; Zygmunt & Buczkowski, 2007**), the density and charge diameter (**Catanach & Hill, 2003**) the way of initiation (**Bohanek et al., 2013; Žganec et al., 2016**) and the charge temperature (**Dobrilović et al., 2014**) on the detonation parameters have been reported. Some authors have tried to improve the detonation properties of ANFO by adding aluminium

(**Maranda et al., 2011; Zygmunt, 2009**) charcoal (**Atlagic et al., 2020**), carbon black (**Izato et al., 2013**), zeolite, and others (**Kuterasiński et al., 2022**).

Given that ANFO is a highly non-ideal explosive, its detonation properties are highly dependent on the charge diameter and confinement characteristics. Knowledge of the detonation parameters of ANFO at different charge diameters and under confinement conditions is of great importance to the mining industry as it helps in tailoring and optimizing the effects of explosives. Unfortunately, experimental data under controlled confinement conditions is sparse and often shows large statistical variations (**Shoch and Nikiforakis, 2014**). The effect of different confinement, such as cardboard, plastic, metals, or different types of rocks, on detonation parameters of ANFO is studied by several researchers (**Arai et al., 2004; Bohanek et al., 2022; Esen, 2004; Jackson et al., 2010, 2011; Souers et al., 2004, Short and Jackson, 2015**). **Eyring et al. (1949)** were the first to propose an equation for the prediction of detonation velocity of confined cylindrical explosive charges. Their equation, which is applicable to thin wall cylinders, considers the charge diameter and explosive to confinement mass ratio per unit length. According to **Souers et al. (2004)** the main shortcoming of Eyring's equation is the fact that it does not consider sound speed in the confining material.

Corresponding author: Vječislav Bohanek
e-mail address: vjecislav.bohanek@rgn.unizg.hr

Eden and Belcher (1989) experimentally studied the effect of sound speed (C_0) on detonation behaviour of TATB-based explosives by constructing a sandwich consisting of a brass plate on one side (C_0=4700 m s⁻¹) and beryllium on the other (C_0=12800 m s⁻¹) and found that the detonation velocity next to the beryllium is about 7% faster. This confirmed the significant influence of the sound speed on the local detonation velocity.

Based on numerical simulation, **Souers et al. (2004)** found two different kinds of wall behaviour, depending on whether the sound speed is faster or slower than the detonation velocity. When the sound speed is faster than the detonation velocity ($C_0 > D$), a shock wave precursor will be created in the wall out ahead of the detonation front next to it. The precursor preshocks the explosive and increases its local detonation velocity (**Souers et al., 2004**). When the sound speed in the wall is slower than the detonation velocity ($C_0 < D$), then a shock wave is created in the wall, transmitting the energy forward and affecting local detonation velocity.

According to **Jackson et al. (2011)**, the net effect of this energy transport on the detonation velocity is still not well understood. For example, the precursor shock can enhance the detonation velocity by precompressing and densifying unreacted explosives near the wall. On the other hand, the precursor shock can change the porosity of the explosive and destroy confinement in front of the detonation wave. The lack of systematic research and high-quality experimental data for mining explosives makes it difficult to pinpoint the effects of the high sound-speed confinement on the detonation properties (**Shoch and Nikiforakis, 2014**).

In this study, the effect of several confining metals detonation properties of ANFO explosive is studied experimentally by measuring the detonation velocity as a function of the charge diameter and the characteristics of the confiner (density and wall thickness), as well as by numerical simulation using hydro-code AUTODYN. The goal of the research is to find a confinement model that will be able to estimate detonation velocity of confined ANFO charges as a function of the charge diameter and characteristics of confinement. In addition, by employing both experimental measurements and simulation, we aim to gain a comprehensive understanding of ANFO detonation behaviour under different confining conditions.

2. Materials and Methods

The study was done on a commercially available ANFO explosive containing 94.6% AN and 5.4% fuel oil, with a minimal oil absorption of 6% and AN prills size ranging between 1.0 and 2.83 mm. The density of the ANFO charges was in the range of 0.76–0.80 g cm⁻³. Metal tubes of different diameters and wall thickness, made of steel, aluminium, and copper were used as the confining materials. The first series of tests was per-

formed using tubes with 37-42 mm diameters and 500 mm length, and the second series using tubes with 75-79 mm diameters and length of 600 mm. The thickness of tube walls varied between 2.0 and 10.25 mm.

2.1. Measurement of velocity of detonation (VoD)

Explosive charges are prepared by pouring ANFO into tubes by taping. The tubes are weighted before and after loading ANFO, and the density of each charge is determined. The charges are initiated by an electric detonator, with a PETN charge of 720 mg of PETN, and an APG20 Mini Booster (90 mm, containing 20 g PETN charge) produced by Austin Powder GMBH. The velocity of detonation was measured by an electrooptical method using Kontinitro EXPLOMET-2 detonating velocity measuring system and fiber optic probes (**Klapötke, 2019**). The distance between the probes was 160 mm. The measurement setup is shown in **Figure 1.**

Figure 1: Measurement setup

2.2. Numerical modelling by AUTODYN

The effect of the confinement characteristics on detonation velocity of cylindrical ANFO charges is simulated by AUTODYN hydro-code. The simulation is carried out using 2D axisymmetric Euler formulation. The size of the elements (axial × radial) was 1x1 mm. The explosive charges are initiated by a 20 g PETN booster charge. Moving gauges are placed along the explosive charge axis (see **Figure 2a**) to register the time of arrival of the detonation wave to determine the detonation velocity (see **Figure 2b**).

The simulation is done using the Lee-Tarver Ignition and Growth (I&G) reactive flow model (**Lee & Tarver, 1980**). The model consists of two Jones-Wilkins-Lee
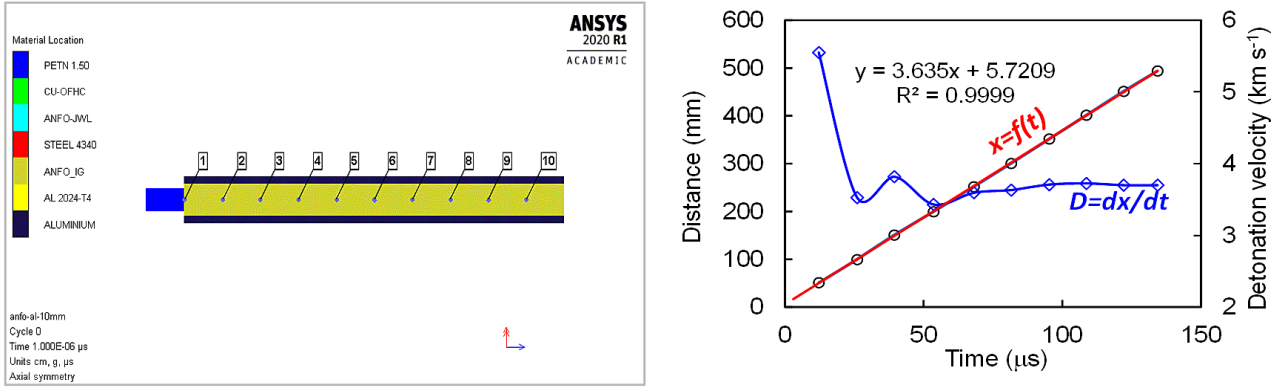
Figure 2: AUTODYN numerical model (**a**) and way of determining detonation velocity (**b**)

(JWL) EOS; one for the unreacted explosive and the other for the reaction products (**Souers et al., 1996**).

$$p = A\left(1 - \frac{\omega}{R_1 V}\right)e^{-R_1 V} + B\left(1 - \frac{\omega}{R_2 V}\right)e^{-R_2 V} + \frac{\omega E}{V} \quad (1)$$

where V is relative volume, E is detonation energy, and A; B, R_1, R_2, and w are constants.

The rate of conversion of unreacted ANFO into detonation products is described by two-term pressure-dependent reaction rate given by equation (2).

$$\frac{\partial F}{\partial t} = I\left(1-F\right)^b \left(\mu - a\right)^x + G\left(1-F\right)^c F^d p^y \quad (2)$$

where F is reacted fraction, p is the pressure, $\mu = \left(\frac{\rho}{\rho_0} - 1\right)$ is the compression and I, a, b, c, d, x, y, G are constants.

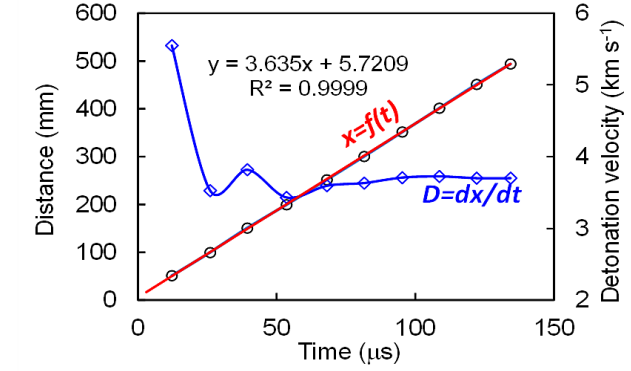Both unreacted and reacted ANFO, and the PETN booster explosive, are described by the JWL EOS. The

JWL EOS parameters for ANFO and the I&G reaction rate parameters are taken from previous work (**Bohanek et al., 2023;**) (see **Table 1**). The JWL parameters for the PETN booster (1.5 g cm⁻³ density) are taken from the AUTODYN material library (**ANSYSInc, 2010**).

The confining materials (steel, copper, and aluminium) are modelled using the material properties from the AUTODYN material library for Steel-4340, CU-OFHC, and AL 6161-T6 (see **Table 2**). These materials correspond most closely to the materials used in the experiments.

3. Results and discussion

3.1. Measurement results

The measured detonation velocities for different tube materials, charge diameters, and different thicknesses of the tubes' walls are summarised in **Table 3**. The results show that for the same thickness of the tube wall, the detonation velocity increases with an increase in the charge diameter. In addition, for the same charge diameter and the tube material, the detonation velocity increases with the thickness of the tube walls. At constant charge diameter and thickness of the tube wall, the detonation velocity is significantly higher for steel than for aluminium tubes. There is not enough data to make a reliable conclusion when it comes to copper tubes, but it appears based on the available data that detonation velocities for copper tubes are slightly higher than for steel tubes (about 5% for w=5 mm).

It was found in our previous work (**Bohanek et al., 2022**) that detonation velocities of confined ANFO charges correlate very well with mC/mE ratio, regardless of the material type. We were able to describe the

Table 1: Input parameters for reacted and unreacted ANFO

Reacted ANFO	Unreacted ANFO, r_0 =0.8 (g cm⁻³)	Lee-Tarver I&G reaction rate parameters
A = 81.6492 GPa	A = 1454.25 GPa	I = 10 ms⁻¹
B = 1.7537 GPa	B = -0.347 GPa	a = 0.2
R_1 = 4.588863	R_1 = 21.8866	b = 0.222
R_2 = 1.021101	R_2 = 0.7874	x = 4
w= 0.32021	w = 3.4613	G = 0.086 ms⁻¹ GPa^-y
D = 4.78 km s⁻¹	E_0 = -0.1549 kJ cm⁻³	c = 0.222
pCJ = 4.61 GPa		d = 0.666
E_0 = 3.448 kJ cm⁻³		y = 0.9
		F_{Igmax} = 0.3

Table 2: Input information for confining materials (**ANSYSInc., 2010**)

Material	Density (g cm⁻³)	EOS	Strength model	Failure model
STEEL 4340	7.83	Linear (K=159 GPa)	Johnson- Cook	Johnson-Cook
CU-OFHC	8.96	Linear (K=129 GPa)	Johnson- Cook	Johnson-Cook
AL 6061-T6	2.703	Shock (g=1.97, C_0=5240 m s⁻¹, s=1.40)	Steinberg-Guinan	none

Table 3: Experimental detonation velocities of ANFO under different confining conditions

No	Confining material	r_C (g cm⁻³)	r_E (g cm⁻³)	d_{in} (mm)	w (mm)	m_C/m_E	D (km s⁻¹)
1			0.80	39	2.8	3.00	2.19
2			0.80	37	7.1	8.44	3.22
3	Carbon steel 1.0308	7.85	0.80	40	10.3	11.31	3.46
4			0.76	79	5.0	3.35	3.72
5			0.76	79	10.0	6.21	4.70
6			0.80	40	2.5	0.82	fail
7			0.80	42	4.0	1.45	1.75
8	Aluminium AlMgSi 0.5	2.70	0.80	40	10.0	4.03	2.54
9			0.76	79	2.5	0.49	2.42
10			0.76	75	5.0	0.95	2.78
11	Copper DHP-Cu	8.93	0.80	40	1.0	0.99	1.66
12			0.80	40	5.0	6.15	2.90

Legend: ρC and ρE are densities of confining material and explosive respectively, d_{in} - inner tube diameter, w – thickness of tube wall, m_C and m_E – mass of metal and explosive per unit length, D – measured velocity of detonation.
Measurements No 1-3, 6-8 and 11-12 are taken from literature (**Bohanek et al., 2022**).

(a)   (b)
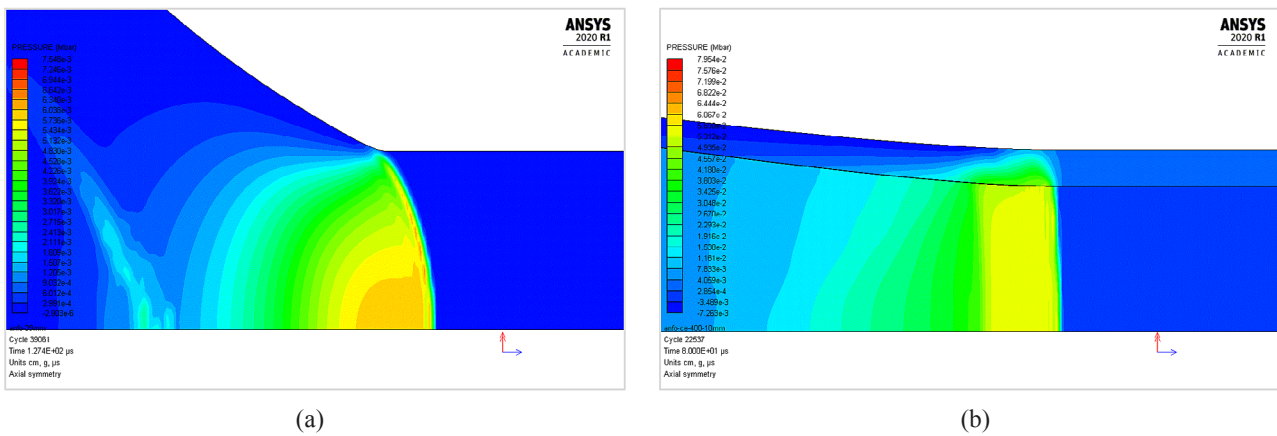
Figure 3: Pressure contours for ANFO charges 80 mm in diameter (**a**) unconfined and (**b**) confined.

dependence of detonation velocity on mC/mE ratio very well by an equation similar to the Gurney's equation used for the estimation of metal liner velocities in the case of cylindrical charges (**Bohanek et al., 2022**). A more detailed analysis of the results is given in the Section 3.3.

3.2. Results of the AUTODYN simulation

The difficulty we faced in designing the experiments was connected to the availability of tubes with all the necessary diameters and wall thicknesses on the market. This resulted in limiting the number of data points required for reliable analysis of $D = f(r_E, r_C, w, d_{in})$ dependence. To overcome this issue, we used AUTODYN simulation to derive additional data points and to extend the range of the tube wall thicknesses. Therefore, the experimentally obtained detonation velocities, supplemented by detonation velocities derived from the AUTODYN simulation, are used in analysis of $D = f(r_E, r_C, w, d_{in})$ dependence. It was found in our previous study (**Bo-** **hanek et al., 2023**) that AUTODYN, with a reactive flow model and parameters given in **Table 1**, can reproduce experimental $D − 1/R_0$ data well for unconfined ANFO, as well as shock initiation and propagation of detonation in confined and unconfined ANFO charges.

Qualitatively different behaviour of unconfined and confined ANFO charges can be clearly observed from the pressure couture graphs shown in **Figure 3**. Unconfined charge shows behaviour typical for highly non-ideal explosives; the existence of a pronounced edge lag (which correlates with the reaction zone length), radial expansion of products in the reaction zone, and a very curved shock front (see **Figure 3a**). Due to radial losses of energy, the detonation velocity of non-ideal explosives is always lower than those predicted by the Chapman-Jouguet theory. In general, the detonation velocity of non-ideal explosives is determined by the interplay between reaction rate and the rate radial expansion.

In the case of a confined charge (see **Figure 3b**), the radial expansion is supressed by the confinement, which
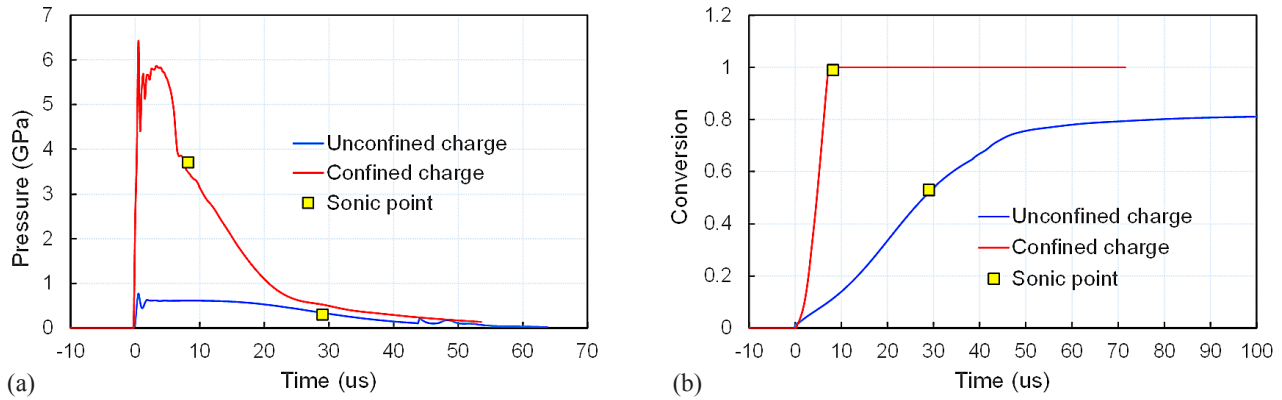
Figure 4: Calculated pressure-time (**a**) and conversion-time (**b**) profiles along longitudinal axis
(Note: Squares represent sonic points, i.e. point where the condition D = up + Co is achieved)
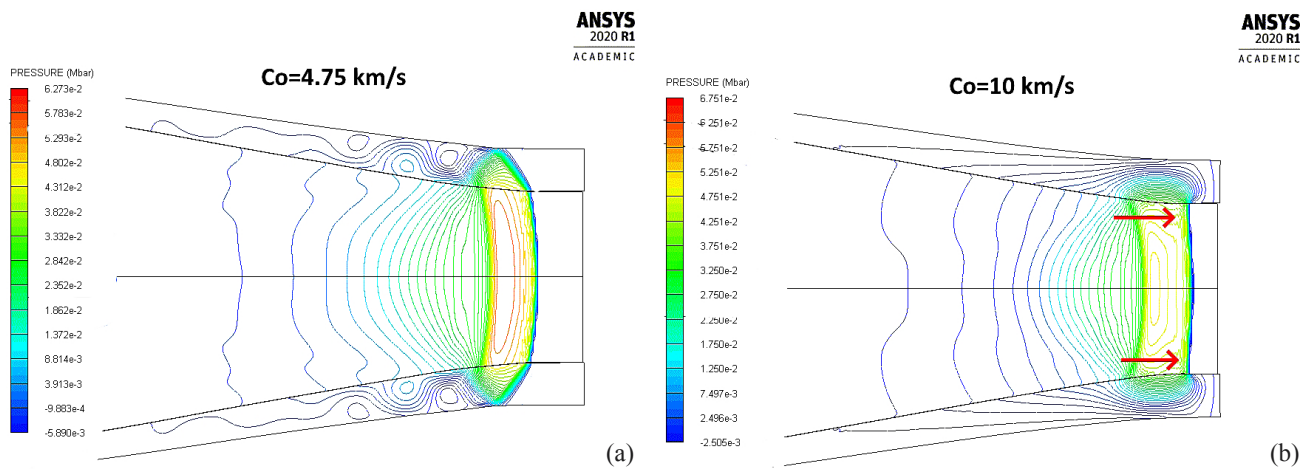

Figure 5: Effect of sound speed on shock front shape a) C_o=4.75 km s^{-1}, b) C_o=10 km s^{-1}

results in a reduction of edge lag and shock front curvature. This, in turn, results in higher detonation velocity and pressure comparing to an unconfined charge. In this specific case (d_{in}=80 mm) calculated unconfined detonation velocity (D_u) equals 1.84 km s^{-1}, and pressure at the sonic point (p_{SP}) equals 0.62 GPa, while the confined detonation velocity (D_c, at w=10 mm thick steel confinement) equals 4.6 km s^{-1} and p_{SP} equals 4.5 GPa (see **Figure 4**).

The suppression of expansion of detonation products results in higher pressure, which in turn results in faster chemical reactions. For illustration, in the case of a confined charge, the reactions along the longitudinal axis are completed after approximately 8 ms (i.e. 24 mm distance from the shock front), while in the case of an unconfined charge only 67% of ANFO reacts at the sonic point (which is reached after 29 ms, i.e. 39 mm). The rest of ANFO continues to decompose beyond the sonic point and after 100 ms, about 20% still remains unreacted.

Both experiments (**Eden and Belcher, 1989**) and hydro-code simulation (**Souers et al., 2004**) have confirmed that sound speed in a tube is an important factor when it comes to the influence of the tube wall on detonation velocity of confined charges. The detonation velocities of the studied ANFO charges range between

1500 and 4600 m s^{-1}, depending on charge radius and wall thickness, which means they are slower than the speed of sound in the confining materials used. Because of that, a shock wave precursor will be created in the wall out ahead of the detonation front next to it, increasing local detonation velocity in ANFO next to the wall. In the case of a confined ANFO charge as shown in **Figure 3b** (d_{in}=80 mm, steel confinement 10 mm thick) the detonation velocity and the sound speed are almost equal (C_0=4.57 km s^{-1} and D=4.60 km s^{-1}). Under such conditions there is no formation of a sharp shock wave in the wall but in the hemisphere of declining pressure, sitting at the metal edge of the detonation front, which agrees with the **Souers et al. (2004)** simulation.

We simulated the effect of sound speed on detonation velocity on an 80 mm diameter charge confined in a 20 mm thick aluminium cylinder. The sound speed varied between 4.75 and 10 km s^{-1} by changing parameters in the shock equation of the state of aluminium. The qualitative effect of sound speed on the shock wave front shape is illustrated in **Figure 5**. For C_0=4.75 km s^{-1} (see **Figure 5a**) the sound speed is close to the detonation velocity (D=4.45 km s^{-1}) and the precursor wave is not created. In contrast, the precursor wave is clearly visible
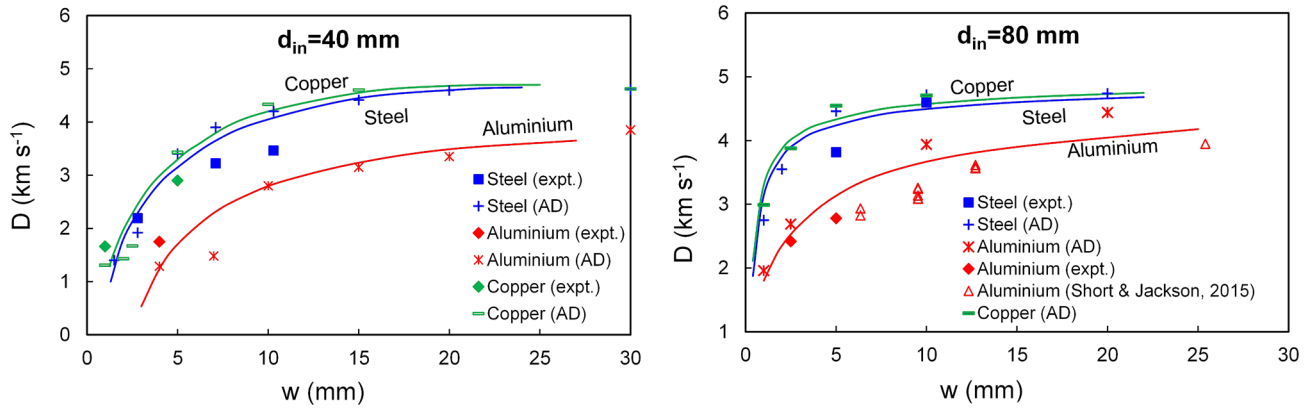
Figure 6: Effect of tube wall thickness and material type on detonation velocity, (**a**) for d_{in}=40 mm and (**b**) d_{in}=80 mm charges (Legend: AD - Autodyn calculation, expt. – experimental result, symbools represent experimental results and Autodyn calculation results)

for C_0 = 10 km s-1 (see **Figure 5b**). The result of the shock wave precursor formation is an increase in local detonation velocity in ANFO near the interface, leading to the formation of a flatter shock front.

However, despite the visible qualitative changes of shock front shape when the sound speed varies, the detonation velocity changes only for 40 m s-1 (around 0.9%) when sound speed changes from 4.75 to 10 km s-1. It should be mentioned that the precursor shock does not initiate a chemical reaction in ANFO (since its pressure is too low- less than 0.15 GPa) but it precompresses ANFO near the interface (density increases from 0.80 to 0.81 g cm3), which can be the reason for a local increase of shock wave velocity. The small increase in detonation velocity is almost within the detonation velocity determination error from the Autodyn simulation, and it cannot be said with certainty that there has been a significant change in detonation velocity with sound speed change.

3.3. Confinement model

The effect of confinement on detonation velocity of ANFO is analysed using the experimental results given in **Table 3**, supplemented with the results derived from the AUTODYN simulation. In addition, data are supplemented with the experimental results of **Short and Jackson (2015)** for aluminium confinement, and the results of **Helm et al. (1976)**, **Lopez et al. (2013)**, **Nyberg et al. (2003)**, and **Sanchindrian et al. (2015)** for copper confinement. By combing experiments and simulation, we covered a wider range of wall thicknesses (up to 30 mm) and got a set of data that we could further process to derive an empirical confinement model. **Figure 6** illustrates the dependence of the detonation velocity on the tube wall thickness for two charge diameters and for different confining materials.

As visible from **Figure 5**, the detonation velocity increases with the wall thickness and reaches the maximum value at a certain wall thickness. For copper and steel tubes the maximum detonation velocity approaches

the ideal detonation velocity (D_{id}= 4.74 km s-1 for r0=0.8 g cm-3), however in the case of aluminium tubes, the maximum detonation velocity is significantly lower than the ideal detonation velocity. This suggests that the ideal detonation velocity cannot be achieved despite an increasing thickness of the wall. At the same time this indicates that, along with the density of the material, its dynamic properties play an important role in thicker tube walls, which makes the effect of confinement on the detonation parameters even more complex. It is obvious that a confinement model that can estimate the detonation velocity of confined charges in a wider range of confining conditions should take into account parameters such as charge diameter, the density of the explosive and the confining materials, and the dynamic properties of the material.

It was also found in **Bohanek et al. (2023)** for the tube walls up to 10 mm thick, the factor that correlates the best with the detonation velocity (at d_{in}=const.) is the mass ratio per of unit length of explosive and confinement (m_E/m_C). **Eyring et al. (1949)** proposed the use of the m_E/m_C ratio to estimate the detonation velocity of confined explosives having different charge radii. The authors proposed the following equation, applicable for thin wall tubes:

$$\frac{D_c}{D_{id}} = 1 - 2.175 \left(\frac{m_E}{m_C} \right) \left(\frac{b}{R_0} \right)^2 \qquad (3)$$

where D_C is the confined detonation velocity, D_{id} is the ideal detonation velocity, R_0 is the charge radius, and b is the fitting constant.

To derive the fitting constant based on our $D=f(R_0, m_E/m_C)$ data, we adapted our in-house non-linear regression analysis code based on the Levenberg-Marquardt method. Preliminary analysis has shown that **Equation 3** cannot satisfactorily describe the $D=f(R_0, m_E/m_C)$ dependence (correlation coefficient was 0.7759 and standard deviation 0.1751km s-1, see **Table 4**). Modifying **Equation 3** by introducing the constant m:

$$\frac{D_c}{D_{id}} = 1 - a \left(\frac{m_E}{m_C} \right)^m \left(\frac{b}{R_0} \right)^2 \tag{4}$$

we obtained a much better correlation (correlation coefficient was 0.7759 and standard deviation 0.1751km s^{-1}, see **Table 4**). The dependence of the detonation velocity on the m_C/m_E ratio (which is the inverse of m_E/m_C) for two different charge diameters is given in **Figure 7.**

Table 4 and **Figure 6** show that **Equation 4** describes the $D=f(R_0, m_E/m_C)$ dependence quite well. Standard deviation for all data points (both experimental and AUTODYN results) is 0.1046, which is reasonably good considering the fact that a number of factors influence the experimental results and the calculated detonation velocity. For example, there is always a certain error in experimentally determined detonation velocity (error of 0.1 km s^{-1} is allowed by standards), AUTODYN simulations predict detonation velocity with a certain error (which can go above 5% for unconfined charges) due to the imperfections of a kinetic model and the equation of state used as well as due to differences in the properties of the confining materials used in the experiments and in the simulation.

Due to the limited number of data available for analysis, it is not possible to reliably determine the range of

m_C/m_E ratios to which the model applies. The maximum m_C/m_E ratio for 80 mm diameter charges was 15, and the model correctly described experimental $D=f(m_C/m_E)$ dependence for all three materials in the analysed range (see **Figure 6b**). For 40 mm diameter charges, where the maximum m_C/m_E ratio analysed was 60, it can be observed that the detonation velocities for aluminium are consistently lower (about 500 m s^{-1}) than that of steel and copper above $m_C/m_E \gg 15$. That leads us to the conclusion that the dynamic properties of the material play an increasingly important role with the increase of the m_C/m_E ratio, which makes the validity of a model above $m_C/m_E \gg 15$ questionable.

A comparison of experimental detonation velocities and velocities derived by the AUTODYN simulation with those predicted by **Equation 4** (using the constants: $a = 1.768422$, $m = 0.575017$, and $b = 14.867955$) is presented in **Figure 8**. The comparison shows that almost all data points for $D > 2$ km s^{-1} lies within $\pm 14.25\%$. The difference expressed as a percentage is much larger for $D < 2$ km s^{-1}, i.e. in the vicinity of the failure radii.

The proposed confinement model can estimate detonation velocity of confined ANFO charges at any charge diameter and for different confining materials. An example is given in **Figure 9**, which shows the change of the detonation velocity of ANFO in a steel tube with an inverse charge radius and the tube wall thickness.

The analysis shows that the estimated and the experimental detonation velocities differ by up to about 400 m s^{-1}. This corresponds to a 10% error at higher detonation velocities and up to 20% at $D=2.0$ km s^{-1}. It should be noted that for $w < 0.5$ mm (which corresponds to $m_C/m_E = 0.28$ at $R_0=35$ mm) calculated $D - 1/R_0$ curve for steel confinement lies below the curve of unconfined ANFO. The same happens for aluminium confinement for $w < 1.3$ mm ($m_C/m_E = 0.26$ at $R_0=35$ mm). The radius of 35 mm roughly corresponds to the failure radius (R_f) of unconfined ANFO (R_f ranges between 32 and 37 mm). This fact limits the lower limit of applicability of the proposed model to $m_C/m_E \gg 0.27$ at $R_0=35$ mm.

Table 4: Fitting constants in Equation 3 and Equation 4

Equation 4 d_{in} = 40 mm (28 data points)	Equation 4 d_{in} = 80 mm (28 data points)	d_{in}=40 and 102 mm (77 data points)	
		Equation 4	**Equation 3**
$a = 1.784458$	$a = 1.991164$	$a = 1.768422$	$a = 2.572061$
$m = 0.558715$	$m = 0.431272$	$m = 0.575017$	
$b = 14.182625$	$b = 15.784044$	$b = 14.867955$	$b = 12.046225$
$s = 0.101$ km s^{-1}	$s = 0.0937$	$s = 0.1046$	$s = 0.1751$
$r = 0.9254$	$r = 0.8499$	$r = 0.8830$	$r = 0.7759$

Note: s is the standard deviation of the estimate, r is the correlation coefficient. R_0 and w are expressed in mm, and m_E and m_C in g mm^{-1}

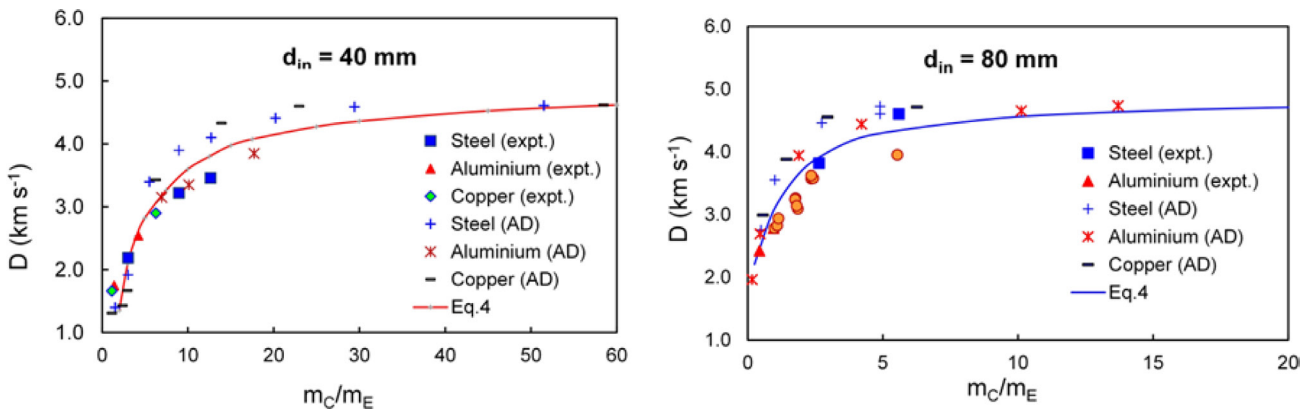**Figure 7:** Dependence of the detonation velocity on m_C/m_E ratio for (a) din=40 mmm and (b) din=80 mm
(Note: solid line represents vales predicted by Equation 4, symbols represent experimental and Autodyn calculation results)
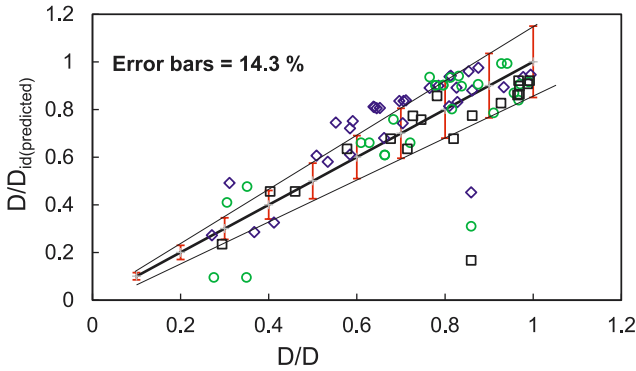
Figure 8: Comparison of experimental and predicted
detonation velocities
(s = 0.1046, r = 0.8830, mean average percentage error
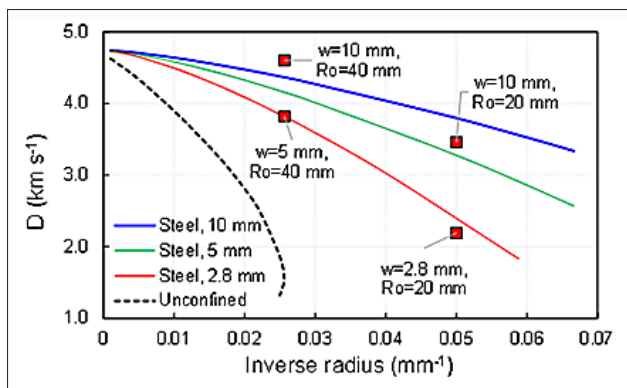(MAPE) = 14.25%)

Figure 9: Estimated detonation velocities of steel confined
ANFO charges vs. inverse charge radius
(squares represent experimental values)

The model predicts that the failure radius of ANFO decreases with the thickness and properties of confining materials. For example, for w =10 mm R_f =8 mm for steel confinement, R_f =14 mm for aluminium, and R_f =20 mm for polyvinylchloride confinement (r_C=1.36 g cm^{-3}).

5. Conclusions

The effect of confinement on the detonation parameters of ANFO explosive was studied experimentally and by numerical simulation using varying charge diameter, confining material type and thickness. The research conclusion can be summarized as follows:

- It was demonstrated that the simulation results agree with the experimental ones, and that both confirm the key role of the mass of the metal to the mass of the explosive ratio (m_C/m_E). For the same charge diameter and thickness of confinement, the confining materials with a higher density (i.e. higher m_C/m_E ratio) result in a higher detonation velocity.
- An empirical confinement model, based on modified Eyring's equation, is proposed. The model enables the estimation of detonation velocities of confined ANFO charges at different charge diameters

and characteristics of confinement, with a mean average percentage error (MAPE) of 14.25%. The model is applicable for thin-wall confinement (i.e. for $0.3 < m_C/m_E < 15$).
- AUTODYN simulation has proven to be an excellent tool for gaining a comprehensive understanding of the non-ideal detonation behaviour of ANFO explosive, as well as explosive-confinement interaction. In addition, with an appropriate reactive flow model, it can generate reliable $D=f(R_0, m_E/m_C)$ data that can be used in the analysis of the confinement effects.
- The AUTODYN simulation showed that varying the speed of sound leads to visible changes in the shape of the shock front of confined ANFO but does not cause a significant change in the detonation speed. The simulation has shown that the ideal detonation velocity of ANFO cannot be achieved solely by increasing the thickness of the confinement, even with an infinite thickness confinement.

6. References

ANSYSInc. (2010): ANSYS Autodyn: User`s Manual: Vol. ISO 9001:2.

Arai, H., Ogata, Y., Wada, Y., Miyake, A., Jung, W. J., Nakamura, J. and Ogawa, T. (2004): Detonation behaviour of ANFO in resin tubes. Science and Technology of Energetic Materials, 65(6), 201–205.

Atlagic, S. G., Biessikirski, A., Kuterasiński, Ł., Dworzak, M., Twardosz, M., Sorogas, N. and Arvanitidis, J. (2020): On the Investigation of Microstructured Charcoal as an ANFO Blasting Enhancer. Energies 2020, Vol. 13, Page 4681, 13(18), 4681. https://doi.org/10.3390/EN13184681

Biessikirski, A., Pytlik, M., Kuterasínski, Ł., Dworzak, M., Twardosz, M. and Napruszewska, B. D. (2020): Influence of the Ammonium Nitrate(V) Porous Prill Assortments and Absorption Index on Ammonium Nitrate Fuel Oil Blasting Properties. Energies 2020, Vol. 13, Page 3763, 13(15), 3763. https://doi.org/10.3390/EN13153763

Bohanek, V., Dobrilović, M. and Škrlec, V. (2013a): Application of explosive energy in metalworking | Primjena energije eksploziva pri obradi metala. Rudarsko Geolosko Naftni Zbornik, 26(1), 29–37.

Bohanek, V., Dobrilović, M. and Škrlec, V. (2013b): Influence of the initiation energy on the velocity of detonation of ANFO explosive. Central European Journal of Energetic Materials, 10(4), 555–568.

Bohanek, V., Štimac Tumara, B., Serene, C. H. Y. and Sućeska, M. (2023): Shock Initiation and Propagation of Detonation

in ANFO. Energies, 16(4). https://doi.org/10.3390/en160 41744

Bohanek, V., Sućeska, M., Dobrilović, M. and Hartlieb, P. (2022): Effect of Confinement on Detonation Velocity and Plate Dent Test Results for ANFO Explosive. Energies, 15(12). https://doi.org/10.3390/en15124404

Buczkowski, D. and Zygmunt, B. (2011): Detonation properties of mixtures of ammonium nitrate based fertilizers and fuels. Central European Journal of Energetic Materials, 8(2), 99–106.

Catanach, R. A. and Hill, L. G. (2003): Diameter Effect Curve and Detonation Front Curvature Measurements for ANFO. 836, 906–909. https://doi.org/10.1063/1.1483684

Dobrilović, M., Bohanek, V. and Žganec, S. (2014): Influence of explosive charge temperature on the velocity of detonation of ANFO explosives. Central European Journal of Energetic Materials, 11(2), 191–197.

Esen, S. (2004): A statistical approach to predict the effect of confinement on the detonation velocity of commercial explosives. Rock Mechanics and Rock Engineering, 37(4), 317–330. https://doi.org/10.1007/s00603-004-0026-3

Eyring, H., Powell, R. E., Duffey, G. H. and Parlin, R. B. (1949): The stability of detonation. Chemical Reviews, 45(1), 69–181. https://doi.org/10.1021/CR60140A002/ ASSET/CR60140A002.FP.PNG_V03

Fabin, M. and Jarosz, T. (2021): Improving ANFO: Effect of Additives and Ammonium Nitrate Morphology on Detonation Parameters. Materials 2021, Vol. 14, Page 5745, 14(19), 5745. https://doi.org/10.3390/MA14195745

Eden, G. and Belcher, R.A. (1989): The Effects of Inert Walls on the Velocity of Detonation in EDC35. The 9th Symposium (International) on Detonation, Oregon, 28 August-1 September 1989, 831-841.

Helm, F., Finger, M., Hayes, B., Lee, E., Cheung, H. and Walton, J. (1976): High explosive characterization for the dice throw event. https://doi.org/10.2172/7267133

Hernandes, V. V., Franco, M. F., Santos, J. M., Melendez-Perez, J. J., Morais, D. R. de, Rocha, W. F. de C., Borges, R., de Souza, W., Zacca, J. J., Logrado, L. P. L., Eberlin, M. N. and Correa, D. N. (2015): Characterization of ANFO explosive by high accuracy ESI(±)–FTMS with forensic identification on real samples by EASI(−)–MS. Forensic Science International, 249, 156–164. https://doi.org/10. 1016/J.FORSCIINT.2015.01.006

Izato, Y. I., Miyake, A. and Date, S. (2013): Combustion characteristics of ammonium nitrate and carbon mixtures based on a thermal decomposition mechanism. Propellants, Explosives, Pyrotechnics, 38(1), 129–135. https://doi.org/10. 1002/PREP.201100106

Jackson, S. I., Kiyanda, C. B. and Short, M. (2010): Precursor detonation wave development in anfo due to aluminum confinement. Proceedings - 14th International Detonation Symposium, IDS 2010, 740–749.

Jackson, S. I., Kiyanda, C. B. and Short, M. (2011): Experimental observations of detonation in ammonium-nitrate-fuel-oil (ANFO) surrounded by a high-sound-speed, shockless, aluminum confiner. Proceedings of the Combustion Institute, 33(2), 2219–2226. https://doi.org/10. 1016/j.proci.2010.07.084

Kavicky, V., Figuli, L., Jangl, S. and Ligasová, Z. (2014): Analysis of the field test results of ammonium nitrate: Fuel oil explosives as improvised explosive device charges. WIT Transactions on the Built Environment, 141, 297–309. https://doi.org/10.2495/SUSI140261

Klapötke, T. M. (2019): 7. Special Aspects of Explosives. Chemistry of High-Energy Materials, 235–268. https:// doi.org/10.1515/9783110624571-007

Kuterasiński, Ł., Wojtkiewicz, A. M., Sadowska, M., Żeliszewska, P., Napruszewska, B. D., Zimowska, M., Pytlik, M., & Biessikirski, A. (2022): Variously Prepared Zeolite Y as a Modifier of ANFO. Materials, 15(17), 5855. https://doi.org/10.3390/MA15175855/S1

Lee, E. L. and Tarver, C. M. (1980): Phenomenological model of shock initiation in heterogeneous explosives. Physics of Fluids, 23(12), 2362–2372. https://doi.org/10.1063/1.862940

López, L. M., Sanchidrián, J. A., Segarra, P. and Ortega, M. F. (2012): Evaluation of ANFO performance with cylinder test. Rock Fragmentation by Blasting: Fragblast 10, 579–586. https://doi.org/10.1201/B13759-82

Maranda, A., Paszula, J., Zawadzka-Małota, I., Kuczyńska, B., Witkowski, W., Nikolczuk, K. and Wilk, Z. (2011): Aluminum powder influence on ANFO detonation parameters. Central European Journal of Energetic Materials, 8(4), 279–292.

Miyake, A., Takahara, K., Ogawa, T., Ogata, Y., Wada, Y. and Arai, H. (2001): Influence of physical properties of ammonium nitrate on the detonation behaviour of ANFO. Journal of Loss Prevention in the Process Industries, 14(6), 533–538. https://doi.org/10.1016/S0950-4230(01)00041-9

Nyberg, U., Arvanitidis, I., Olsson, M. and Ouchterlony, F. (2003): Large size cylinder expansion tests on ANFO and gassed bulk emulsion explosives. *EXPLOSIVES AND BLASTING TECHNIQUE*, 181–191.

Short, M. and Jackson, S. I. (2015): Dynamics of high sound-speed metal confiners driven by non-ideal high-explosive detonation. Combustion and Flame, 162(5), 1857–1867. https://doi.org/10.1016/J.COMBUSTFLAME.2014.12.007

Sanchidrián, J. A., Castedo, R., López, L. M., Segarra, P., and Santos, A. P. (2015): Determination of the JWL Constants for ANFO and Emulsion Explosives from Cylinder Test Data. Central European Journal of Energetic Materials, 12(Vol. 12, 2), 177--194

Schoch S. and Nikiforakis N. (2014): Propagation of detonation waves in ANFO confined by high sound-speed materials, Proc. Of 15th International Detonation Symposium, San Francisco, CA, July 13-18, 2014, 1031-1041.

Souers, P. C., Vitello, P., Esen, S., Kruttschnitt, J. and Bilgin, H. A. (2004): The Effects of Containment on Detonation Velocity. Propellants, Explosives, Pyrotechnics, 29(1), 19–26. https://doi.org/10.1002/prep.200400028

Souers, P. C., Wu, B., & Haselman, L. C. Jr. (1996): Detonation equation of state at LLNL, 1995. Revision 3. https:// doi.org/10.2172/204120

Tumara, B. Š., Dobrilović, M., Škrlec, V. and Sućeska, M. (2022): Determination of detonation front curvature radius of anfo explosives and its importance in numerical modelling of detonation with the wood-kirkwood model.

Rudarsko-Geološko-Naftni Zbornik, 37(2), 97–107. https://doi.org/10.17794/RGN2022.2.9

Žganec, S., Bohanek, V. and Dobrilović, M. (2016): Influence of a primer on the velocity of detonation of ANFO and heavy ANFO blends. Central European Journal of Energetic Materials, 13(3), 694–704. https://doi.org/10.22211/cejem/65017

Zygmunt, B. (2009): Detonation parameters of mixtures containing ammonium nitrate and aluminium. Central European Journal of Energetic Materials, 6(1), 57–66.

Zygmunt, B. and Buczkowski, D. (2007): Influence of ammonium nitrate prills' properties on detonation velocity of ANFO. Propellants, Explosives, Pyrotechnics, 32(5), 411–414. https://doi.org/10.1002/prep.200700045

SAŽETAK

Utjecaj materijala obloge na detonacijske parametre ANFO eksploziva

S obzirom na dobru učinkovitost miniranja, sigurnost i cijenu, ANFO eksploziv najčešće je korišteni eksploziv za civilnu primjenu. ANFO eksploziv tipičan je predstavnik neidealnih eksploziva, što znači da njegova detonacijska svojstva jako ovise o promjeru punjenja te postojanju i svojstvima obloge. U radu se eksperimentalno i simulacijom pomoću hidrokoda proučava utjecaj različitih materijala obloge na detonacijska svojstva ANFO eksploziva mijenjanjem promjera naboja te vrste i debljine obloge. Rezultati pokazuju da uz promjer naboja ključan utjecaj na detonacijska svojstva imaju gustoća i debljina materijala obloge. Predložen je empirijski model obloge, primjenjiv u rasponu od 0,3 < mC/mE < 15. Model omogućuje procjenu brzine detonacije ANFO naboja s oblogom od različitih materijala sa srednjom apsolutnom postotnom pogreškom (MAPE) od 14,25 %.

Ključne riječi:
eksplozivi, ANFO, obloga, detonacija, AUTODYN, model obloge

Authors' contribution

Vječislav Bohanek (1) (PhD., Associate Professor) performed testing, presentation, and interpretation of the test results. **Muhamed Sućeska (2)** (PhD., Professor) performed the ANSYS AUTODYN simulation, presentation, and interpretation of the results. **Ivana Dobrilović (3)** (PhD., Post-doctoral Researcher) performed calculation, simulation, and interpretation of the results. **Paulo Pleše (4)** (MSc.) participated in site testing and interpretation of the results.